

# Growth of pure zinc blende p-type GaAs nanowires by metal-organic chemical vapor deposition\*

Li Ran(李然)<sup>1,†</sup>, Huang Hui(黄辉)<sup>1,2,†</sup>, Ren Xiaomin(任晓敏)<sup>1</sup>, Guo Jingwei(郭经纬)<sup>1</sup>, Liu Xiaolong(刘小龙)<sup>1</sup>, Huang Yongqing(黄永清)<sup>1</sup>, and Cai Shiwei(蔡世伟)<sup>1</sup>

<sup>1</sup>Key Laboratory of Information Photonics and Optical Communications, Ministry of Education, Beijing University of Posts and Telecommunications, Beijing 100088, China

<sup>2</sup>Electronics Science and Technology Institute, Dalian University of Technology, Dalian 116085, China

**Abstract:** Vertical p-type gallium arsenide (GaAs) nanowires with pure zinc blende structure were grown on GaAs (111) B substrate by metal-organic chemical vapor deposition via a Au-catalyst vapor-liquid-solid mechanism. The p-type doping was investigated by additional diethyl zinc (DEZn). In the high II/III ratio range (II/III > 9.1%), there exists a critical length beyond which kinking takes place. Two possible reasons are discussed. Zn occurrence in the nanowires was verified by energy dispersive X-ray (EDX) analysis. Corresponding to II/III = 0.2%, the doping concentration is about  $8 \times 10^{18} \text{ cm}^{-3}$ .

**Key words:** GaAs nanowire; p-type doping; metal organic chemical vapor position; zinc-blende structure

**DOI:** 10.1088/1674-4926/32/5/053003

**PACC:** 0130; 0220; 7280E

## 1. Introduction

Semiconductor nanowires (NWs) are ideal building blocks for a functional nanoscale device<sup>[1–3]</sup>. P-type doping is essential for the nanoscale device. However, systematic studies on reliable and well-controlled doping are still lacking for semiconductor nanowires.

As reported, there are three major p-type dopant atoms in GaAs nanowires: Zn<sup>[4,5]</sup>, C<sup>[6]</sup> and Be<sup>[7,8]</sup>. As for C<sup>[6]</sup>, adding CBr<sub>4</sub> to the gas phase will corrode the nanowires. For Be<sup>[7,8]</sup>, it is usually as a p-type dopant precursor in a molecular beam epitaxy (MBE) system. In principle, there are two possible ways to incorporate active dopants into nanowires<sup>[5]</sup>: (a) doping during the growth process<sup>[4,6–8]</sup>; and (b) post growth doping via diffusion or ion implantation<sup>[5]</sup>. However, for postgrowth doping via implantation and annealing, a number of  $\sim 5 \times 10^9 \text{ cm}^{-2}$  dislocations were observed in the dark-field image. The dislocations resulted from the recrystallization process<sup>[5]</sup>.

In this paper, Au-catalyst vapor-liquid-solid (VLS)<sup>[9]</sup> growth of stacking-faults-free zinc blende p-type GaAs nanowires on GaAs (111) B substrate were investigated by using DEZn as a dopant precursor during the growth process. The nanowires were characterized with the following techniques: scanning electron microscopy (SEM), transmission electron microscope (TEM) and energy dispersive X-ray (EDX) analysis.

## 2. Experiment

The epitaxy was performed by metal organic chemical vapor deposition (MOCVD) with a Thomas Swan CCS-MOCVD

system at a pressure of 100 Torr<sup>[10,11]</sup>. Growth of P-GaAs nanowire was carried out in the following steps. (1) a 4 nm Au layer was deposited on the substrate by magnetron sputtering. Then the Au-coated GaAs (111) B substrate was loaded into a MOCVD reactor and annealed in situ at 650 °C under arsine ambient for 300 s to form Au–Ga alloy particles as a catalyst. (2) H<sub>2</sub> was used as the carrier gas. Trimethyl gallium (TMGa) and arsine (AsH<sub>3</sub>) were used as precursors at a constant V/III ratio of 70. Simultaneously, DEZn as doping precursor was injected into the reactor cell. (3) Nanowires were grown for 500 s at a growth temperature of 440 °C. Samples A, B and C's II/III ratio was 18.1%, 9.1%, 0.2%, respectively.

In step (3), low temperature growth can reduce planar defects and lateral overgrowth<sup>[12,13]</sup>, and the growth condition including temperature and V/III ratio is previously optimized.

Atom force microscopy (AFM) was used to analyze the density of the Au–Ga particles after the annealing process. The morphologies of the nanowires were characterized by a Hitachi S-5500 SEM. The crystal structure of the nanowires was investigated by a Jeol-2100F TEM, which operates at 300 kV. TEM specimens were prepared by ultrasonic nanowires in ethanol for 5 min and then dispersing them onto holey carbon grids.

## 3. Results and discussion

Figures 1, 2, and 4 show the SEM images of samples A, B and C, respectively. In every figure, (a)–(d) show the vertical view, 20° inclination view and cross-sectional view of NWs. For samples A and B (depicted in Figs. 1, 2), nanowires are non-uniform in diameter and length. In Fig. 1(d), kinking takes place in the 389 nm position, while in Fig. 2(d), the kinking

\* Project supported by the National Basic Research Program of China (No. 2010CB327601), the Key International Cooperation Research Project of the National Natural Science Foundation of China (No. 90201035), the Chinese Universities Scientific Fund (No. BUPT2009RC0410), the National Natural Science Foundation of China (No. 61077049), and the 111 Program of China (No. B07005).

† Corresponding author. Email: liranbupt@gmail.com; huihuang@bupt.edu.cn

Received 12 October 2010, revised manuscript received 2 December 2010

© 2011 Chinese Institute of Electronics

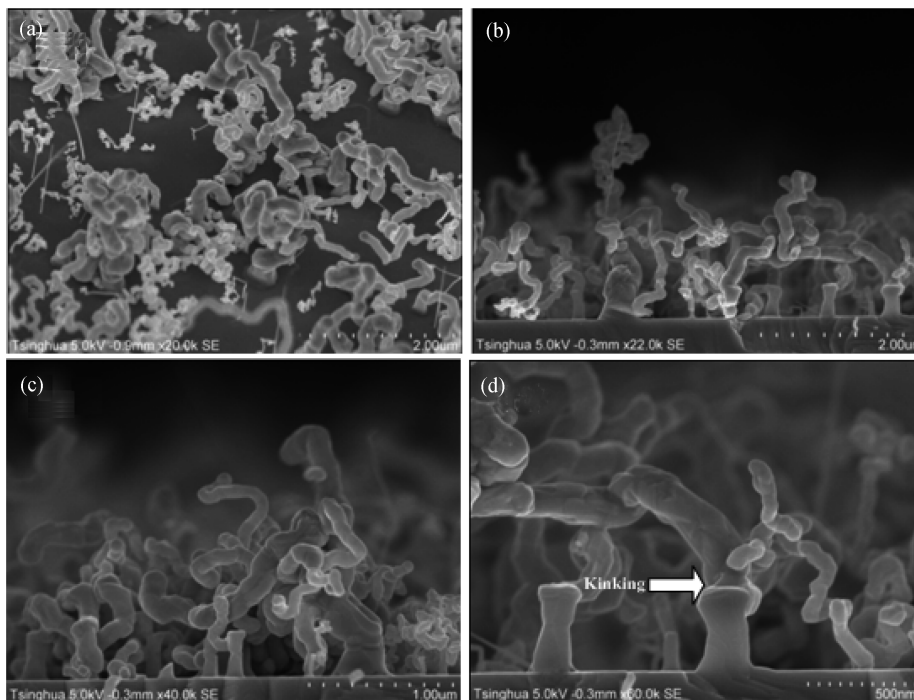


Fig. 1. SEM images of sample A (II/III = 18.1%). (a) Vertical view. (b) Cross-sectional view, scale bar = 2 μm. (c) Cross-sectional view, scale bar = 1 μm. (d) Cross-sectional view, scale bar = 500 nm.

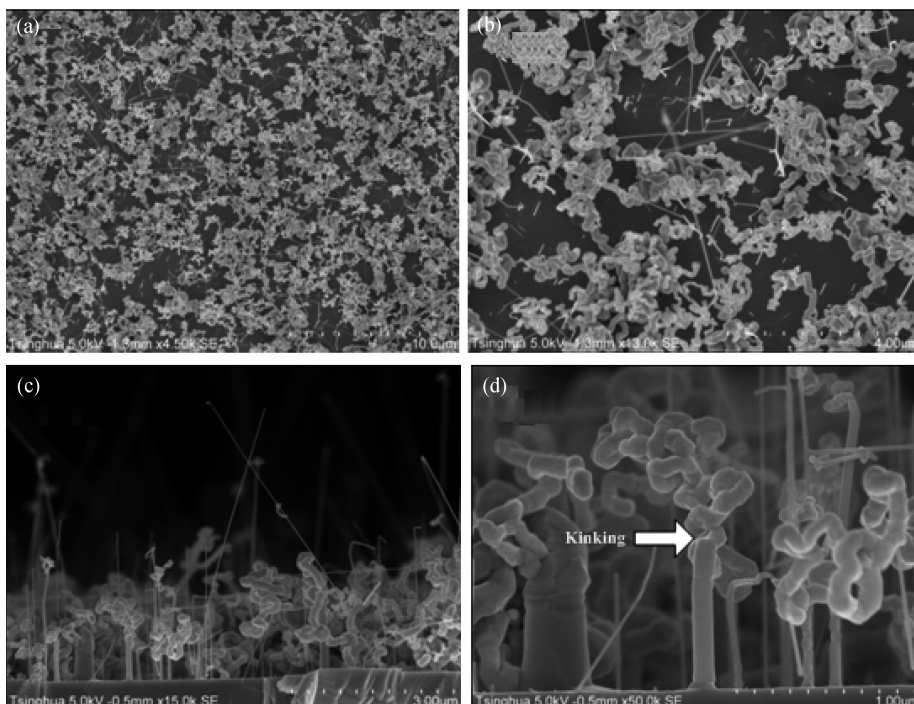


Fig. 2. SEM images of sample B (II/III = 9.1%). (a) Vertical view. (b) 3 times magnification, scale bar = 4 μm. (c) Cross-sectional view, scale bar = 3 μm. (d) Scale bar = 1 μm, and the arrow indicates the kinking place.

location is 838 nm. Two possible reasons may influence the bending of p-GaAs nanowires. (1) Excess Zn atoms may segregate on the sidewalls forming the deformation area<sup>[7]</sup>. The comparison experiment kinking before and after (as shown in Fig. 3 and Table 1) can demonstrate that the Zn concentration has increased after kinking. (2) Surface stress and surface elasticity effects as He and Lilley reported in Ref. [14]. In the high

II/III ratio range (II/III > 9.1%), corresponding to each II/III ratio, there exists a critical length beyond which bending takes place. This value increases with decreasing II/III ratio. It is an interesting phenomenon that the stump is perpendicular to the substrate but the trunk is distorted. As reported by Gutsche *et al.*<sup>[4]</sup>, good structural properties of p-GaAs NW growth is up to a II/III ratio of 0.4%, while at a higher II/III ratio wire

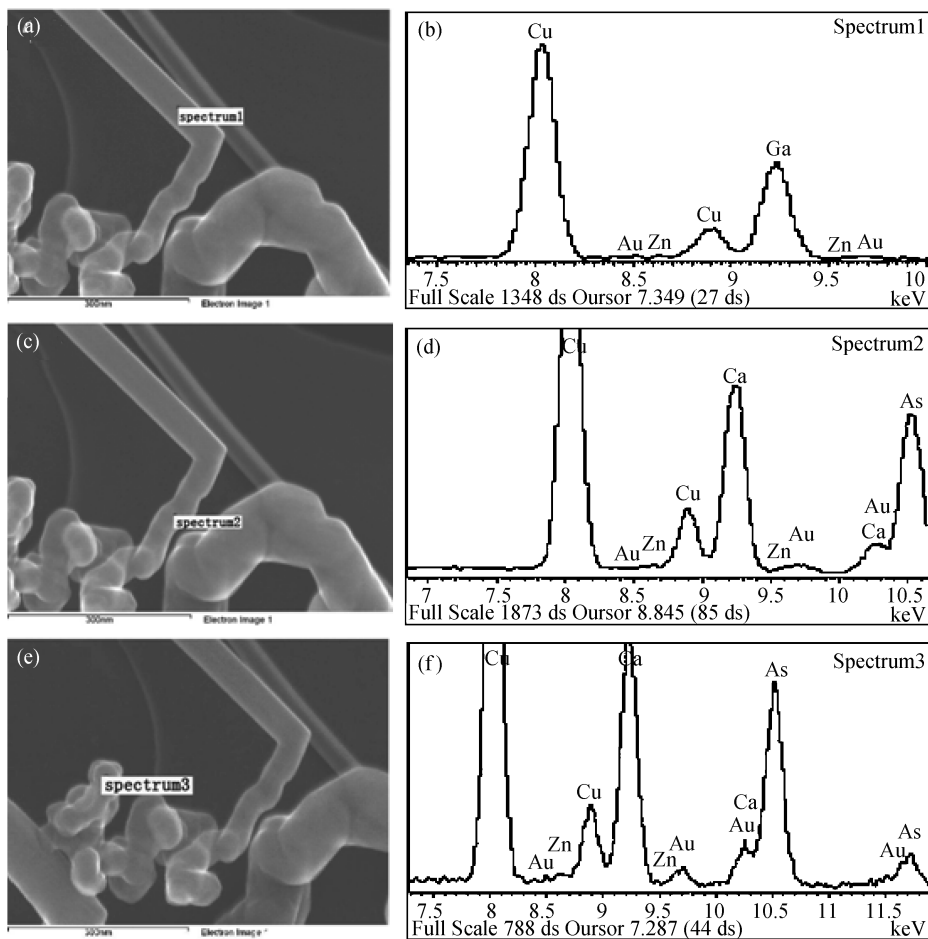


Fig. 3. Zn concentration comparison between kinking (a) before and (c) (e) after.

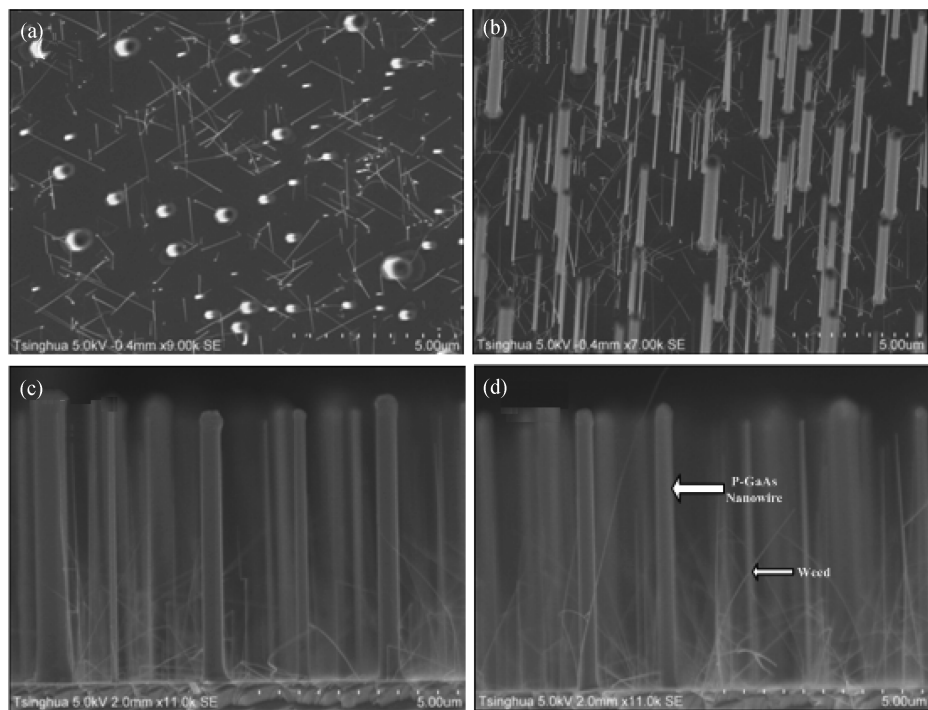


Fig. 4. SEM images of sample C (II/III = 0.2%). (a) Vertical view. (b) 20° inclination view, scale bar = 5 μm. (c) Cross-sectional view, scale bar = 5 μm. (d) Cross-sectional view, scale bar = 5 μm, and the upper arrow indicates well-grown nanowires and the lower arrow indicates weeds.

Table 1. EDX comparison between spectra 1, 2 and 3.

Element	Weight % (Spectrum 1)	Weight % (Spectrum 2)	Weight % (Spectrum 3)
Ga	21.7	24.6	24
As	78.2	75.1	75.6
Zn	0.1	0.3	0.4
Total	100	100	100

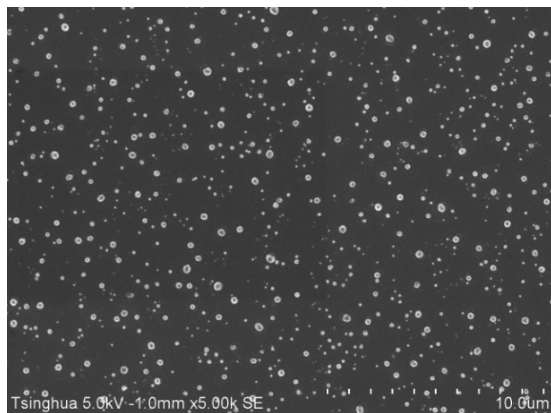


Fig. 5. AFM images of Au–Ga particles annealed from gold film.

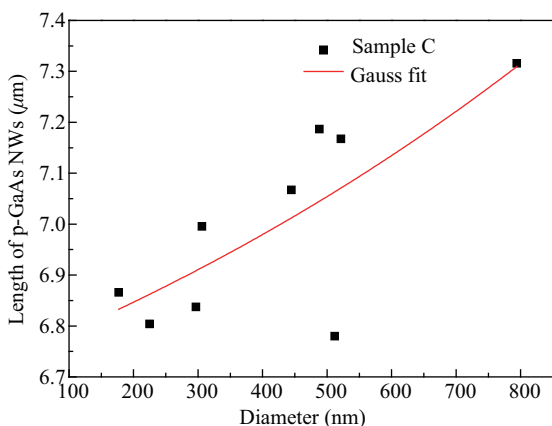


Fig. 6. Correlation between the length and diameter of sample C.

kinking. So far, our experiments have also proved this point.

For sample C (as shown in Fig. 4), nanowires whose morphology is cylindrical clavate are perpendicular to the substrate. They are uniform in diameter and length. We make statistics of sample C. The average length is 6.84  $\mu\text{m}$ , and the corresponding growth rate is 13.68 nm/s. The average diameter of the nanowires is 418.2 nm, and the density of the nanowires is about  $10^9 \text{ cm}^{-2}$ , which is based on the Au–Ga alloy particle density (as shown in Fig. 5). Through the statistics, 80% of the nanowires are perpendicular to the substrate, (i.e. grow along the [111] direction). The p-GaAs NWs length is plotted as a function of diameter (shown as Fig. 6). The black spot denotes each concrete data and the red curve indicates the Gauss fit curve. From Fig. 6, it can be concluded that the p-GaAs nanowires' length is proportional to the diameter in the investigated range.

Nanowires of Sample C are uniform in diameter. There are two major reasons to explain this phenomenon. (1) Low growth

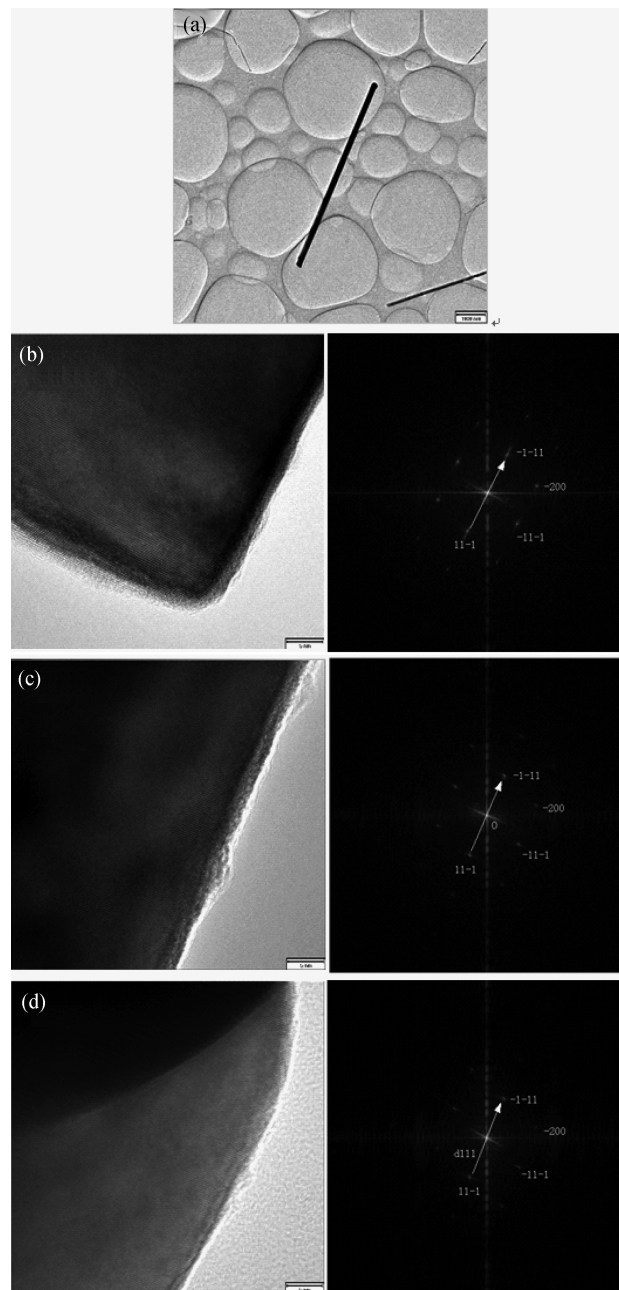


Fig. 7. TEM analysis of a NW with a diameter of 228 nm. (a) Bright field TEM image, scale bar = 1000 nm. (b) HRTEM image of the stump, scale bar = 5 nm. (c) HRTEM image of the middle section, scale bar = 5 nm. (d) HRTEM image of an alloy particle capped wire tip. The right diagrams indicate the corresponding Fourier transform of the (b), (c) and (d) structure.

temperature (such as 440  $^{\circ}\text{C}$ ) results in untapered structures<sup>[15]</sup>. (2) Speaking from the mechanism of nanowire growth, there are two major supply atoms, that is, the ones of the precursor which directly impinge onto the alloy droplet and the other ones called adsorb atoms which diffuse from sidewalls and substrate<sup>[10,16–19]</sup>. Studies show that adsorb atoms will result in lateral overgrowth and tapering. For sample C, under high V-group saturation conditions, adsorb atoms are restrained, while atoms of precursors are dominant.

Figure 7 shows the TEM analysis of a wire from sample C with a diameter of 228 nm and the TEM images are taken with



Fig. 8. High-resolution TEM image of the nanowire with a diameter of 228 nm.

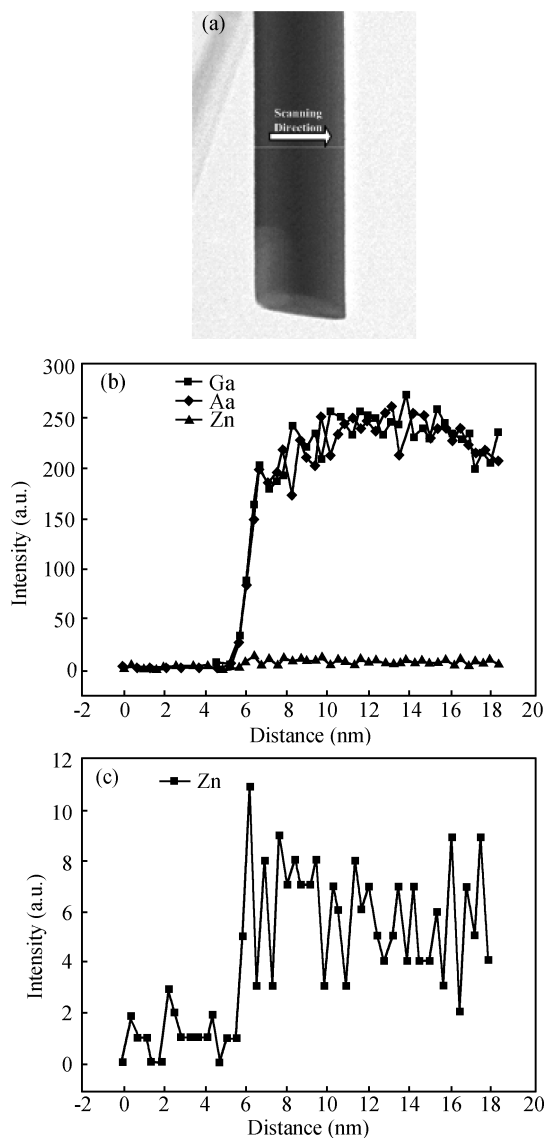


Fig. 9. EDX analysis of NW from sample C. (a) The arrow refers to the radial scanning direction. (b) Element detection chart. (c) Individual Zn element detection chart.

$[0\bar{1}\bar{1}]$  direction of the electron beam incidence. For Figs. 7(b), 7(c), and 7(d), the right graph is the corresponding Fourier transform of the left structure. The objective function in positive space has a Fourier transform to obtain a diffracted wave in reciprocal space<sup>[20]</sup>. Therefore the right graph is also the corresponding selected-area diffraction (SAD) and the bright spot denotes a homologous crystal plane. High-resolution TEM (HRTEM) images of the stump, middle section and top can testify that there are no defects, such as stacking faults and twinning superlattices in the nanowire.

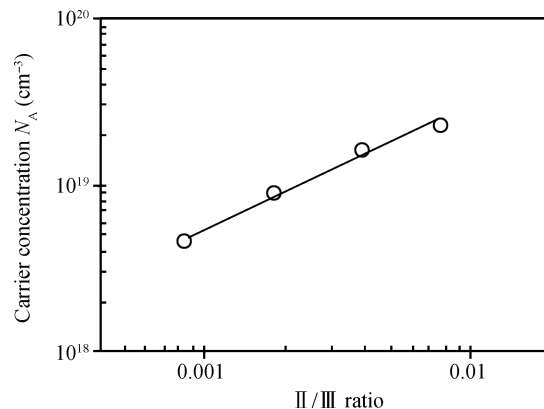


Fig. 10. Linear graph of the doping concentration and II/III ratio (Re. Journal of Applied Physics 2009).

From the HRTEM image (as shown in Fig. 8), p-GaAs nanowire is composed of a series of Ga atomic layers and As atomic layers (i.e. double atomic layers)<sup>[21]</sup>. Each atomic layer is a (111) facet, so we can measure the spacing interval between the (111) facets and the result is  $d_{111} = 0.375$  nm, according to the following equation<sup>[20]</sup>,

$$d_{hkl} = \frac{a}{\sqrt{h^2 + k^2 + l^2}}$$

$$\Rightarrow a = d_{hkl} \sqrt{h^2 + k^2 + l^2}. \quad (1)$$

Here,  $a$  is the lattice constant and  $h, k, l$  represent the crystal plane indices. For the (111) facet,  $h = 1, k = 1, l = 1$ , so the lattice constant  $a = d_{111} \times \sqrt{2} = 0.375 \times \sqrt{2} = 0.5303$  nm. This value is close to the GaAs bulk materials' lattice constant  $a = 0.565325$  nm. Based on this, it can be inferred that the nanowire is a pure zinc-blende structure.

Figure 9 shows the EDX analysis of a nanowire (from sample C) with a diameter of 228 nm. As shown in Fig. 9(b), the maximum count of the Ga, As, Zn element is 263, 249, 11, respectively, so it can be summarized that the Zn element is nominal compared to the Ga, As element. For clarity, the individual Zn element detection chart (just as Fig. 9(c)) is made, and the variety of Zn element along the radial direction could further prove its existence. Gustsche *et al.*<sup>[4]</sup> have reported that the Zn acceptor density is proportional to the II/III ratio. In addition, an almost linear behavior between the DEZn flow and the Zn concentration was demonstrated in the investigated range. This characteristic is depicted in Fig. 10. Corresponding to II/III = 0.2%, the doping concentration is about  $8 \times 10^{18} \text{ cm}^{-3}$ .

#### 4. Conclusions

In summary, pure zinc blende stacking-fault-free p-type GaAs nanowires were investigated by using DEZn during the growth process. The growth mechanism, crystal structure, and correlation between diameter and length were studied. In the high II/III ratio ( $\text{II/III} > 9.1\%$ ), there exists a critical length beyond which kinking takes place. Two possible reasons may influence the bending of p-GaAs nanowires (1) Excess Zn atoms may segregate on the sidewall forming deformation area. The comparison experiment of Zn concentration has been made.

(2) Surface stress and surface elasticity effects. Corresponding to II/III = 0.2%, the acceptor Zn concentration is about  $8 \times 10^{18} \text{ cm}^{-3}$ .

## Acknowledgment

The authors thank V. G. Dubrovskii (Lofte Physical Technical Institute of the Russian Academy of Sciences) for fruitful collaborations.

## References

- [1] Wang J, Gudiksen M S, Duan X, et al. Highly polarized photoluminescence and photodetection from single indium phosphide nanowires. *Science*, 2001, 293: 1455
- [2] Li Y, Qian F, Xiang J, et al. Nanowire electronic and optoelectronic devices. *Materials Today*, 2006, 9(10): 18
- [3] Pauzauskis P J, Yang P D. Nanowire photonics. *Materials Today*, 2006, 9(10): 36
- [4] Gutsche C, Regolin I, Blekker K, et al. Controllable p-type doping of GaAs nanowires during vapor–liquid–solid growth. *J Appl Phys*, 2009, 105: 024305
- [5] Stichtenoth D, Wegener K, Gutsche C, et al. P-type doping of GaAs nanowires. *Appl Phys Lett*, 2008, 92: 163107
- [6] Vinaji S, Lochthofen A, Mertin W, et al. Material and doping transitions in single GaAs-based nanowires probed by Kelvin probe force microscopy. *Nanotechnology*, 2009, 20: 385702
- [7] Cirlin G E, Bouravleuv A D, Soshnikov I P, et al. Photovoltaic properties of p-doped GaAs nanowire arrays grown on n-type GaAs (111) B substrate. *Nanoscale Res Lett*, 2010, 5: 360
- [8] Ihn S G, Ryu M Y, Song J I. Optical properties of undoped, Be-doped, and Si-doped wurtzite-rich GaAs nanowires grown on Si substrates by molecular beam epitaxy. *Solid State Commun*, 2010, 150: 729
- [9] Wagner R S, Ellis W C. Vapor–liquid–solid mechanism of single crystal growth. *Appl Phys Lett*, 1964, 4: 89
- [10] Huang H, Ren X M, Ye X, et al. Growth of stacking-faults-free zinc blende GaAs nanowires on Si substrate by using Al-GaAs/GaAs buffer layers. *Nano Lett*, 2010, 10: 64
- [11] Ye X, Huang H, Ren X M, et al. Growth of pure zinc blende GaAs nanowires: effect of size and density of Au nanoparticles. *Chin Phys Lett*, 2010, 27(4): 046101
- [12] Bao X Y, Soci C, Susac D, et al. Heteroepitaxial growth of vertical GaAs nanowires on Si (111) substrates by metal-organic chemical vapor deposition. *Nano Lett*, 2008, 8: 3755
- [13] Joyce H J, Gao Q, Tan H H, et al. Twin-free uniform epitaxial GaAs nanowires grown by a two-temperature process. *Nano Lett*, 2007, 7: 921
- [14] He J, Lilley C M. Surface effect on the elastic behavior of static bending nanowires. *Nano Lett*, 2008, 8(7): 1798
- [15] Paiano P, Prete P, Lovergine N, et al. Size and shape control of GaAs nanowires by metalorganic vapor phase epitaxy using tertiarybutylarsine. *J Appl Phys*, 2006, 100: 094305
- [16] Lu W, Lieber C M. Semiconductor nanowires. *J Phys D: Appl Phys*, 2006, 39: R387
- [17] Plante M C, Lapierre R R. Au-assisted growth of GaAs nanowires by gas source molecular beam epitaxy: tapering, sidewall faceting and crystal structure. *J Cryst Growth*, 2008, 310: 356
- [18] Soci C, Bao X Y, Aplin D P R, et al. A systematic study on the growth of GaAs nanowires by metal-organic chemical vapor deposition. *Nano Lett*, 2008, 8: 4275
- [19] Dubrovskii V G, Sibirev N V, Cirlin G E, et al. Gibbs-Thomson and diffusion-induced contributions to the growth rate of Si, InP, and GaAs nanowires. *Phys Rev B*, 2009, 79: 205316
- [20] Huang X Y. *The microstructure of materials and its electron microscopy analysis*. 3rd ed. Beijing: Metallurgical Industry Press, 2008 (in Chinese)
- [21] Liu N K, Zhu B S, Luo J S. *Semiconductor physics*. Beijing: Electronics Industry Press, 2008 (in Chinese)